Journal of Membrane Science and Research 5 (2019) 11-19

Journal of Membrane Science & Research

journal homepage: www.msrjournal.com

Research Paper

A Comparative Study on the Application of Porous PES and PEI Hollow Fiber Membranes in Gas Humidification Process

Gholamreza Bakeri *

Advanced Membrane Technology Research Lab, Faculty of Chemical Engineering, Babol Noshirvani University of Technology, Babol, Iran

Article info

Received 2017-08-30
Revised 2018-05-23
Accepted 2018-05-27
Available online 2018-05-27

Keywords

Humidification
Polyetherimide
Polyethersulfone
Hollow fiber membrane
Membrane contactor

Highlights

- Two different PES and PEI hollow fiber membranes were fabricated and applied in gas humidification process.
- Effects of different operating conditions on the performance of membranes in humidification process were studied.
- Even though the skin layer of PES membrane is more porous but the water flux of PEI membrane is higher.
- The structure of membrane sublayer has critical role in humidification process as the pore condensation occurs in narrow regions of membrane sublayer and declines the water flux.

Graphical abstract

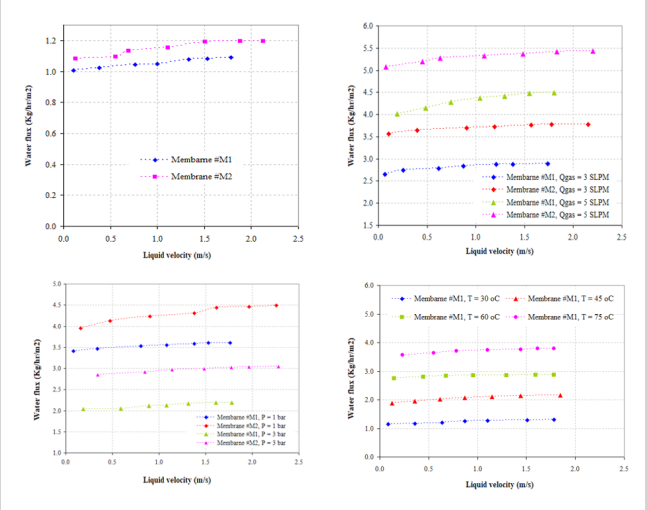

Abstract

Humidification process is one of the applications of membrane contactor systems in which partial pressure of a vapor in the gas stream increases. In this study, two different polyethersulfone and polyetherimide hollow fiber membranes were fabricated and characterized by various test methods and their performance in humidification process under different operating conditions was investigated. The PES membrane has more porous skin layer which its mean pore size and gas permeance are 191% and 566% more than PEI membrane, respectively but its porosity is lower that can be related to its more spongelike structure and higher concentration of the polymer at the cloud point. On the other hand, the water vapor flux of PEI membrane is higher than PES membrane that can be related to the difference in the sublayer structure of the membranes which causes water vapor to condense along the pores of the membrane. Furthermore, the difference in water vapor fluxes between PEI and PES membrane increases as the operating pressure/liquid temperature increases that may be related to the intensification of pore condensation phenomenon. The results of this research show that the structure of membrane sublayer has critical effect on the vapor flux in the humidification process.

1. Introduction

Gas humidification process has widely been used in petrochemical and chemical industries in which the vapor pressure of a liquid is increased in a gas stream e.g., in fuel cell applications, the relative humidity of the reactant gases is essential to make the proton exchange membrane (PEM) more effective; therefore the reactant gases are generally saturated with water vapor before entering the fuel cell chamber.

Traditionally, bubbling of the gas in the liquid (generally hot liquid) is used and the vapor is carried by the gas stream. For example, in formaldehyde production process, air is bubbled in a vessel of hot methanol and the air/methanol mixture is sent to the reactor. This process has some drawbacks such as low efficiency, high pressure drop [1], entrainment of liquid droplet and low contact area between the gas and liquid streams that necessitates the application of huge equipments [2].

Several processes have been proposed to overcome the aforementioned difficulties such as steam generation [3], spray towers [4] and ultrasonic humidification. Humidification of gas, based on enthalpy wheel system was proposed by Casalegno et al. [5] where heat and humidity are transferred simultaneously from the exit gas of the fuel cell to the inlet gas through a

* Corresponding author at: Phone: +98 912 526 5739; fax: +98 11 323 34 204
E-mail address: bakeri@nit.ac.ir (Gh. Bakeri)

DOI: 10.22079/JMSR.2018.71014.1156

rotating ceramic wheel, even though some fluctuations are created in the system due to the rotation of wheel. Furthermore, optimization of this system is not easy that is related to the number of effective parameters.

Spraying of the liquid in the packed bed column is another method for humidification of gas where the gas and liquid enter to the column from the top and the bottom of the column, respectively while the column is filled with packing. Even though this process makes low pressure drop for the gas, long tower, difficulties in selection of suitable packing and maintenance of the tower limit the application of this process [6].

Membrane based processes have been suggested for humidification of the gas [7] that offer some advantages such as higher efficiency and less energy consumption [8], high modularity, easier control of the process, lower pressure drop, smaller equipments etc. [9]. In this process, a membrane (porous or nonporous) is located between the gas and liquid streams where the liquid vapor diffuses through the membrane pores to reach the gas phase [10, 11].

In case of nonporous membrane, the membrane has a dense skin layer that governs the transfer of liquid to the gas stream. The liquid should dissolve firstly in the skin layer and then penetrate through the membrane; therefore the polymer that is used for the fabrication of membrane should be selected based on its affinity to the liquid [12]. Traditionally, Nafion based nonporous membranes are used for increasing the relative humidity of gases in the fuel cell applications which show high mechanical stability and water uptake [13] but their price is high (e.g. 500 $ m^{-2}) [11, 14]. The application of Nafion membrane in humidification process and developing a model for water permeation through the membrane was done by Park and Oh [15]. The water permeation through solvent-resistant polyimide dense membrane was investigated by Huang et al. [16]. The application of dense Nafion membrane in gas humidification process was studied by Merida and Cave [17]. Performance comparison between porous and nonporous membranes in humidification process was studied by Park et al. [11] where they used porous PSf and Nafion flat sheet membranes in a humidifier. Even though the price of Nafion membranes is much higher than PSf membrane (at least 50 times more), the performance of porous membrane is 2-10 times more than Nafion membrane.

The arrangement of membrane in the membrane contactor depends on the type of the membrane as for flat sheet membrane, the parallel-plate membrane contactor is the common one [18] in which the gas and liquid flow in counter-flow or cross-flow regime. Furthermore, in case of hollow fiber membrane, the membranes are arranged in a tube and were potted at both ends which the arrangement of the contactor is similar to shell-and-tube heat exchanger [7, 19, 20]; the liquid can flow in the shell or through the lumen side of the contactor.

In porous membrane [21, 22], the mechanism of mass transfer is by diffusion of the molecules through the gas filled pores of the membrane i.e. the liquid evaporates at the entrance of the pores, the vapor diffuses through the pores and enters the gas stream at the other end of the pores. Since the liquid should not enter the pores of the membrane, membranes with low wettability (e.g. hydrophobic membranes [23]) are applied in humidification process. Even though penetration of liquid in the pores of the membrane decreases the diffusion length of the vapor, it further reduces the rate of heat transfer to the liquid along the pores and declines the evaporation rate. Furthermore, the wettability of membrane can be reduced by adjusting the pore size of the membrane which enables the non-hydrophobic membranes to be used in the humidification process [21].

As the vapor diffuses through the pores of the porous membrane and there is no dense skin layer on the surface of the membrane, the performance of porous membranes in humidification process is much higher than nonporous membrane. The characteristics of porous membrane such as pore size, membrane porosity, surface porosity etc. are effective on the vapor flux. Furthermore, the resistance of the membrane against the penetration of liquid prevents the decline in vapor flux during long term operation, even though partial wettability of membrane decreases the performance of the membrane, mainly at the beginning of the process [24].

The objective of this study is to apply two different polyetherimide (PEI) and polyethersulfone (PES) hollow fiber membranes in gas humidification process and comparing their performance at various operating conditions and study the effect of operating parameters on the water vapor flux. PEI and PES membranes have good thermal and chemical resistance and have been applied in membrane gas absorption process [25, 26] which showed reasonable results; therefore it is expected that PEI and PES membranes present suitable performance in humidification process. Furthermore, comparing the characteristics of membranes provides the criteria to find the ones that govern the performance of the membrane in the humidification process.

2. Experimental

2.1. Materials

Polyethersulfone (PES, UDEL ™) and polyetherimide (PEI, Ultem®) as the base polymers for fabrication of hollow fiber membranes were purchased from ARKEMA and General Electric companies, respectively and were dried overnight at 70 ºC before dissolution in the solvent. N-methyl-2-pyrrolidone (NMP) with the purity of 99.5 wt% was purchased from Merck and was used as the solvent. Distilled water was used as the nonsolvent additive to PES solution.

2.2. Preparation of spinning solution

The polymers were dissolved in NMP at 70 ºC under gentle mixing to make the polymer solution with desired concentration. The compositions of the polymer solutions are presented in Table 1.

Table 1
The compositions of polymer solutions.

Material (wt%)	#1	#2
PES concentration (wt%)	15	-
PEI concentration (wt%)	-	12
NMP concentration (wt%)	81	88
Nonsolvent concentration (wt%)	4	-

In case of PES solution (#M1), the nonsolvent additive (water) was added to the polymer solution where a white solid was formed and then was dissolved by gentle mixing.

2.3. Fabrication of hollow fiber membranes

Nonsolvent induced phase inversion (NIPS) method was used for fabrication of the membranes. The fabrication conditions are presented in Table 2 and the details of spinning process were reported elsewhere [27].

Table 2
The conditions for membrane fabrication.

Parameter	Membrane #M1	Membrane #M2
Bore fluid	Water	Water
Bore fluid temperature	Room temperature	Room temperature
Coagulant bath temperature	Room temperature	Room temperature
Air gap (cm)	1	0

After spinning, the wet spun hollow fibers were immersed in the water bath for a few days to take out the residual solvent and then were dried naturally by hanging at room temperature.

2.4. Measurement of the cloud point and viscosity of polymer solutions

The thermodynamic stability and the viscosity of polymer solution are two parameters that affect on the mechanism of phase inversion process. The method for cloud point measurement was described in detail elsewhere [26]; briefly the quantity of water that is required to make the polymer solution cloudy was measured. The viscosity of polymer solutions was measured by viscometer, EW-98965-40, Cole Parmer, USA.

2.5. Fabrication of membrane module for gas permeation test

Gas permeation test is a common test for measuring the effective surface porosity and mean pore size of the membrane [28] and is used for comparing the membranes that are used in contactor applications. One end of some hollow fiber membranes with specified length were potted in a stainless steel tubing while the other end of the fibers was closed by epoxy resin. The gas permeation module and the system used for gas permeation test are shown in Figure 1.

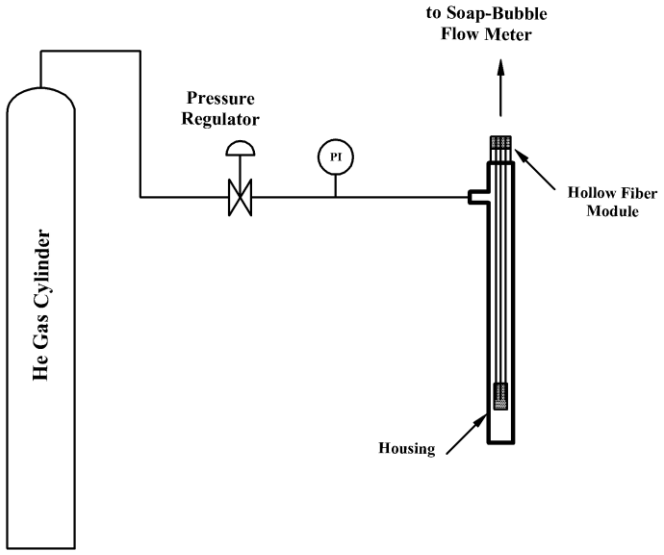

Fig. 1. The schematic of hollow fiber membrane module and gas permeation test system.

In gas permeation test, the helium gas flows through the shell side of the membrane module and the pressure of the gas is increased with a step size of 0.5 bar; at each pressure, the flow rate of the permeated gas is measured by soap bubble flow meter. The permeation rate of the helium gas is calculated based on the outer surface area of the hollow fiber membranes.

Assuming the pores of the membrane to be straight and cylindrical and the gas flows through the pores of the membrane under Knudsen and Poiseuille flow regimes, the total gas permeation rate is calculated by Eq. 1.

$$\bar{P} = P_K + P_P = \frac{2}{3}\left(\frac{8RT}{\pi M}\right)^{0.5}\frac{r_{P,m}}{RT}\frac{\xi}{L_P} + \frac{1}{8\mu}\frac{r_{P,m}^2}{RT}\frac{\xi}{L_P}\bar{p} = A + B\bar{p} \quad (1)$$

where $\bar{P}$ is the total gas permeance (mol m^{-2} Pa^{-1} s^{-1}), P_K and P_P are the gas permeation rate under Knudsen and Poiseuille flow regimes, respectively (mol m^{-2} Pa^{-1} s^{-1}), T is the absolute temperature (K), M is the molecular weight of the gas (Kg mol^{-1}), R is the universal gas constant (8.314 J mol^{-1} K^{-1}), $r_{p,m}$ is the mean pore radius (m), ξ is the surface porosity (the ratio of A_P to A_T where A_P is the area of the pores and A_T is the total area of the membrane), μ is the gas viscosity (Pa.s), L_P is the effective pore length (m) and $\bar{P}$ is the mean pressure (Pa) (that is $\frac{p_u + p_d}{2}$ where P_u is the upstream pressure and P_d is the downstream pressure). Therefore, the plot of total gas permeance versus mean pressure should be a straight line and the slope (A) and intercept (B) of the line are used in Eqs. 2 and 3 to calculate the effective surface porosity and mean pore size of the membrane.

$$\frac{\xi}{L_P} = \frac{8\mu RTB}{r_{P,m}^2} \quad (2)$$

$$r_{P,m} = \frac{16}{3}\frac{B}{A}\left(\frac{8RT}{\pi M}\right)^{0.5}\mu \quad (3)$$

2.6. Membrane porosity and tortuosity

The membrane porosity (ε) is a measure of the void volume in the structure of the porous membrane and influence on the permeation flux in contactor applications. The method for porosity measurement was described elsewhere in detail [29] where the length and weight of wet and dry membrane were measured and used for calculation of membrane porosity. The tortuosity of membrane (τ) is calculated by Eq. 4 and is a criterion of the actual length of the pores; the higher the tortuosity of membrane, the higher the mass transfer resistance of membrane.

$$\tau = \frac{(2-\varepsilon)^2}{\varepsilon} \quad (4)$$

2.7. Liquid entry pressure of water (LEPw) test

Penetration of the liquid into the pores of membrane influence on the mass transfer through the membrane; therefore the resistance of the membrane against the wettability should be measured. In liquid entry pressure of water test, the liquid is pushed to the lumen side of the membrane and the pressure of the liquid is increased with a step size of 0.2 bar; the pressure that the first droplets of water appear on the outer surface of the membrane is reported as LEPw. Even though the biggest pores wet at first, LEPw is a suitable criterion for the resistance of membrane against the wettability.

2.8. Scanning electron microscopy (SEM) analysis

SEM analysis was used to observe the structure of the membrane. The fibers were fractured in the liquid nitrogen and then platinum sputtered. The SEM micrographs of the membrane cross section were taken.

2.9. Gas humidification test

The performance of the fabricated membranes in gas humidification process was evaluated in terms of the water vapor flux and enhancement in the relative humidity of the gas. The specifications of the membrane contactor modules, used in the humidification process is presented in Table 3 and the schematic of the gas humidification system is shown in Figure 2 where the dry gas (N_2) was sent to the shell side of the contactor while its mass flow rate (in terms of standard liter per minute (SLPM)) was controlled by mass flow controller (MFC, model: Alborg DFC26). The pressure of the gas was controlled by the valve at the exit of the contactor. Distilled water was warmed by the heater in the tank to the specified temperature and was sent to the lumen side of the contactor. The pressure of the liquid was adjusted 0.5 bar higher than the pressure of the gas. The flow rate of the liquid was changed by the valve at the exit of the contactor.

The relative humidity and temperature of the exit gas were measured by the humidity analyzer (model: Lutron LM 8000) and the water vapor flux was calculated using the mass flow rate of the dry N_2 gas, the temperature and the relative humidity of the exit gas.

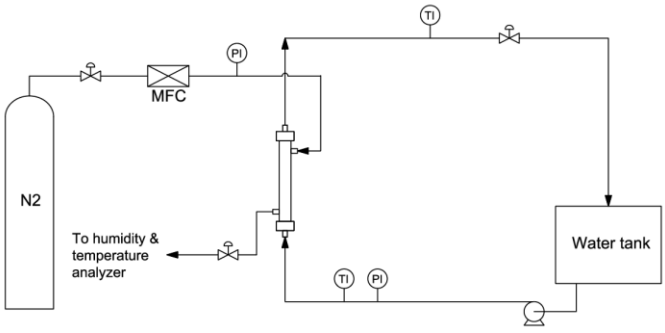

Fig. 2. Schematics of the humidification system, TI: temperature indicator, PI: pressure indicator, MFC: mass flow controller.

Table 3
The specifications of contactor module used in humidification process.

Parameter	#M1	#M2
D_{shell}	1 cm	
Effective length of contactor	18 cm	
Number of fibers	4	5
Gas	Pure N_2	
Liquid	Distilled water	
T_{gas} (inlet)	Room temperature	

3. Results and discussion

3.1. Morphological studies

The cloud point and viscosity tests results are shown in Table 4. In addition, the concentration of the polymer (PES or PEI) at the cloud point, which can influence on the membrane porosity, was calculated using the concentration of the polymer solutions and the amounts of the coagulant (water) that is required to reach the cloud point.

Table 4
The cloud point and viscosity tests results for the polymer solutions.

Solution No.	g water / 100 g polymer solution	Polymer (wt%) at cloud point	Polymer solution viscosity (cP)
#M1	7.50	13.96	216.8
#M2	4.53	11.48	201.8

Cloud point test results show that PES solution is more stable thermodynamically than PEI solution even though the concentration of PES solution is higher and nonsolvent additive was added to the PES solution; that is associated to the characteristics of the polymers. Furthermore, the concentration of the polymer at the cloud point for PEI solution is lower that can enhance the porosity of the fabricated membrane. The viscosity of the polymer solutions is nearly the same; the parameter that affect on the intrusion rate of the external/internal coagulants into the structure of nascent fibers. On the other hand, the hydrophilicity of the polymers are different that will affect on the phase inversion process.

The SEM micrographs for the cross section and outer surface of the fabricated membranes are shown in Figure 3 where both membranes show porous skin layer, sublayer with fingerlike macrovoids that extend from the outer and inner surfaces of the membrane to the middle of membrane cross section and a small area with spongelike structure in the middle of the cross section, that is related to the slow phase inversion process; this spongelike area is more pronounced in membrane #M1. The low viscosity of the polymer solutions causes fast intrusion of the internal and external coagulants into the structure of nascent fiber that makes the macrovoids [30].

Since dry jet-wet phase inversion method was used for the fabrication of membrane #M1, the VIPS (Vapor Induced Phase Inversion) process makes a nascent skin layer on the outer surface of the membrane that can hinder the penetration of coagulant; the lower length of macrovoids originating from the outer surface of the membrane #M1 can be related to this phenomenon (see Figure 3). Furthermore, the polymer solution #2 is more unstable thermodynamically than polymer solution #1. However, the characteristics tests results for the fabricated membranes (Table 5) show that membrane #M1 has bigger mean pore size (191% higher) and higher gas permeation rate (566% higher), i.e. the skin layer of the membrane #M1 is more porous that may be related to the higher hydrophilicity of PES solution that makes more intrusion of coagulant into the structure of nascent fiber. On the other hand, membrane #M2 has higher porosity that can be related to the lower concentration of polymer at the cloud point. The higher porosity of membrane #M2 provides lower tortuosity that reduces the effective diffusion length of the vapor through the membrane. The LEPw test results show that membrane #M1 has lower wettability, i.e. the size of the biggest pores on the surface of membrane #M1 is smaller than membrane #M2 and the pore size distribution of membrane #M2 is wider than membrane #M1.

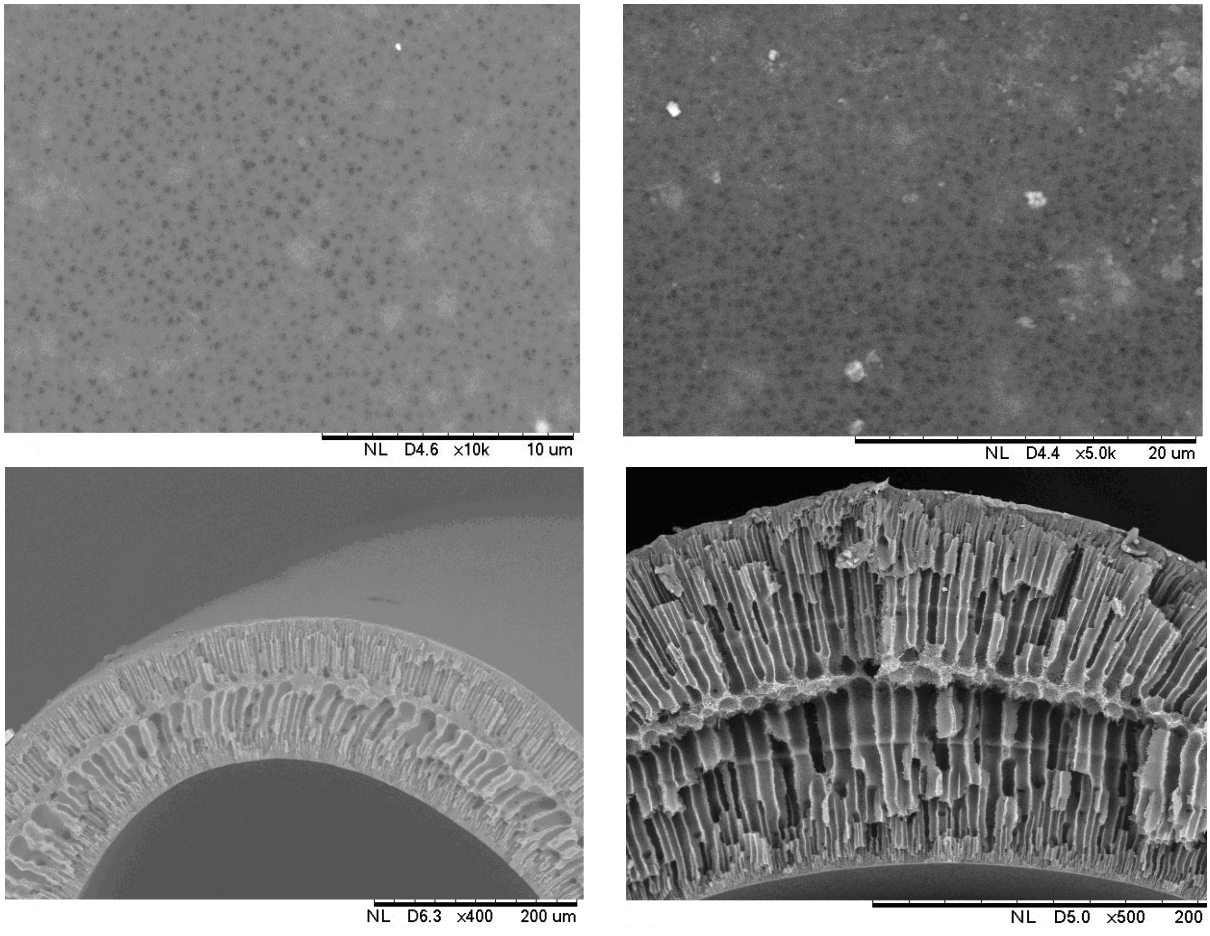

Fig. 3. SEM micrographs of membranes' cross section and outer surface: (a) membrane #M1 and (b) membrane #M2.

Table 5
The characterization test results of the fabricated membranes.

Membrane No.	Mean pore size, $r_{p.m}$ (nm)	Effective surface porosity (m^{-1})	Helium gas permeance @ 1 bar ($\frac{cm^3 (STP)}{cm^2\ cmHg\ s}$)	Liquid entry pressure of water (LEPw) (bar)	Membrane porosity	Membrane tortuosity	ID/OD of HFM (mm)
#M1	653	28	0.0304	4.2	0.805	1.77	0.50/0.81
#M2	224.5	15	0.0046	3.0	0.831	1.65	0.46/0.78

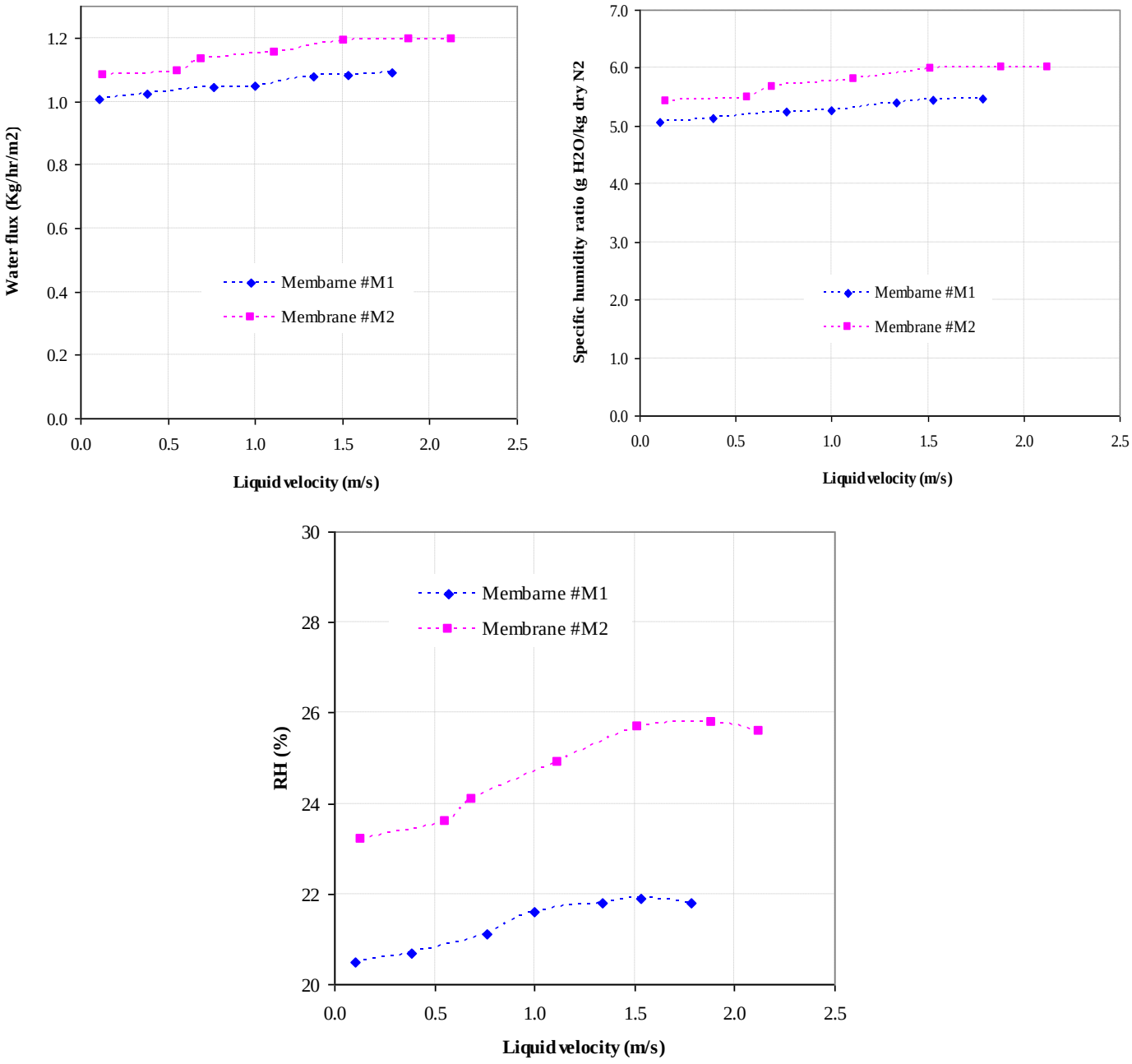

Fig. 4. Plots of water flux, specific humidity ratio and relative humidity of the exit gas versus liquid velocity for the fabricated membranes; Q_{gas} = 3 SLPM, T = 30 °C, P = 3 bar.

3.2. The effect of liquid velocity

The effect of liquid velocity on the water vapor flux (in terms of kg m^{-2} hr^{-1}), specific humidity ratio (in terms of g water/kg dry N_2) and relative humidity of the exit gas are presented in Figure 4 where all terms improve with the liquid velocity. Since the liquid is pure in the humidification process, there is no mass transfer boundary layer in liquid side [31] and the total mass transfer resistance depends on the membrane and gas side resistances. On the other hand, the vaporization of liquid at the entrance of the pores needs energy transfer from the bulk of the liquid. Therefore, temperature

polarization affects on the liquid temperature profile in the vicinity of the membrane; the higher the liquid velocity the thinner the thermal boundary layer. For liquid velocities more than a specific value (V_c), the temperature polarization effect is negligible and the plot of vapor flux levels off [8, 23] as is shown in Figure 4. The lower the membrane/gas side mass transfer resistance or the higher the liquid temperature, the higher the V_c.

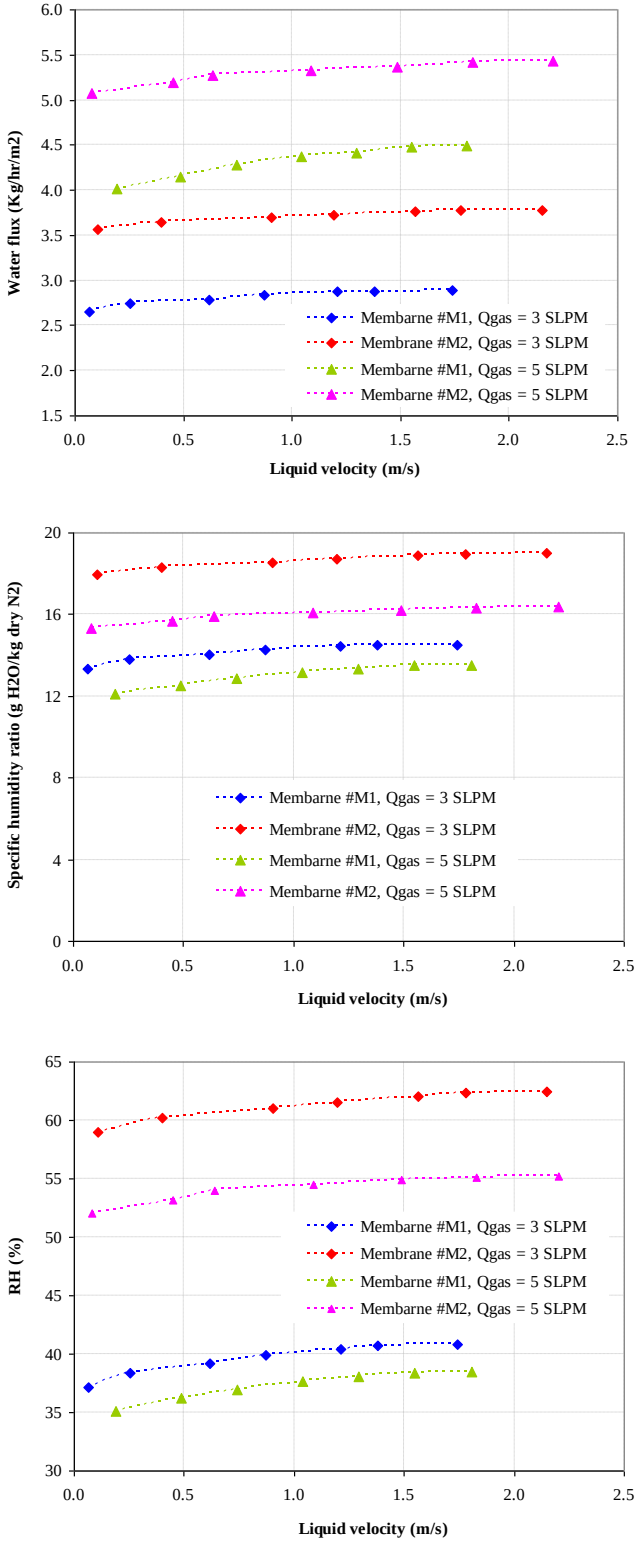

Fig. 5. Plots of water flux, specific humidity ratio and relative humidity of the exit gas at different dry gas flow rates for the fabricated membranes, T = 75 °C, P = 3 bar.

3.3. The effect of gas flow rate

The water flux at different dry gas (N_2) flow rates are presented in Figure 5 where both membranes illustrate better water flux at higher gas flow rate that is due to the reduction in gas side mass transfer resistance [7, 31, 32]. On the other hand, the specific humidity ratio and relative humidity of the exit gas decreases as the gas flow rate increases that is related to the dilution of water vapor in the gas stream at higher gas flow rate even though the water flux increases [11, 23].

3.4. The effect of operating pressure

Increasing the operating pressure increases the partial pressure of water vapor and reduces the capacity of the gas for water vapor; as a result, the driving force for the liquid vaporization decreases [22]. Furthermore, the diffusivity of water vapor through the pores of the membrane decline as the operating pressure increases. Therefore, the water flux, specific humidity ratio and relative humidity of the exit gas diminish with the pressure (see Figure 6). Furthermore, the water flux of membrane #M2 is higher than membrane #M1 where at higher pressure, the difference in water flux between membrane #M2 and membrane #M1 is more.

3.5. The effect of liquid temperature

The plots of water flux, specific humidity ratio and relative humidity of the exit gas at different liquid temperatures are presented in Figure 7 where the increase in liquid temperature enhances all terms, as was reported elsewhere [7, 8, 12, 23]. Furthermore, the water flux of membrane #M2 is more and the difference between these membranes in terms of water flux increases at the higher temperatures.

Increasing the liquid temperature enhances the vapor pressure (according to Antoine equation) and reduces the heat of vaporization of the liquid, i.e. more vapor is generated at the entrance of the pore. Furthermore, higher liquid temperature increases the temperature of the gas stream and enhances the saturation pressure of the gas, i.e. higher capacity of the gas for water vapor. In addition, increasing the liquid temperature diminishes the thickness of thermal boundary layer on the surface of membrane and improves the heat transfer. Increasing the liquid temperature further enhances the diffusivity of liquid vapor molecules along the membrane pores which has positive effect on the water flux.

The temperature plots for the exit gas at two different liquid temperatures are presented in Figure 8. There are two mechanisms for heat transfer to the gas stream, 1- energy transfer by the vapor transmitted to the gas, 2- throughout the membrane body by the conduction. Even though the water flux of membrane #M2 is higher than membrane #M1, the trend for the temperature of the exit gas is reverse that may be due to the higher thermal conductivity of PES membrane.

Assuming exponential correlation between the water vapor flux and the temperature of the liquid (Eq. 5), the activation energy of humidification process can be calculated by plotting Ln F versus $1/T$, which should be a line.

$$F = F_0 \exp(-\frac{E}{RT}) \quad (5)$$

where F is the water flux (kg m^{-2} hr^{-1}), R is the universal gas constant (J mol^{-1} K^{-1}), E is the activation energy (J mol^{-1}) and T is the temperature of the liquid (K). The plots were drew at different liquid velocities (a sample plot at V_{liquid} = 2 m s^{-1} is shown in Figure 9) for each membrane and the calculated activation energies were averaged that are presented in Table 6.

The CO_2 absorption fluxes of the fabricated PEI (membrane #M2) and PES (membrane #M1) hollow fiber membranes were reported elsewhere [25,26] where PES hollow fiber membrane showed higher CO_2 absorption flux than PEI membrane that can be correlated to its characteristics such as bigger mean pore size and higher LEPw, e.g. in case of V_{liquid} = 1.5 m s^{-1}, the CO_2 absorption flux of membrane #M1 is 71% higher than membrane #M2. However, the results of this study show that PEI membrane has higher water vapor flux and it can be concluded that other parameters can affect on the performance of membrane in humidification process, which will be discussed as follows.

Table 6
The average activation energies (kJ/mol) for the fabricated membranes in humidification process.

Membrane #M1	Membrane #M2
20.53	18.73

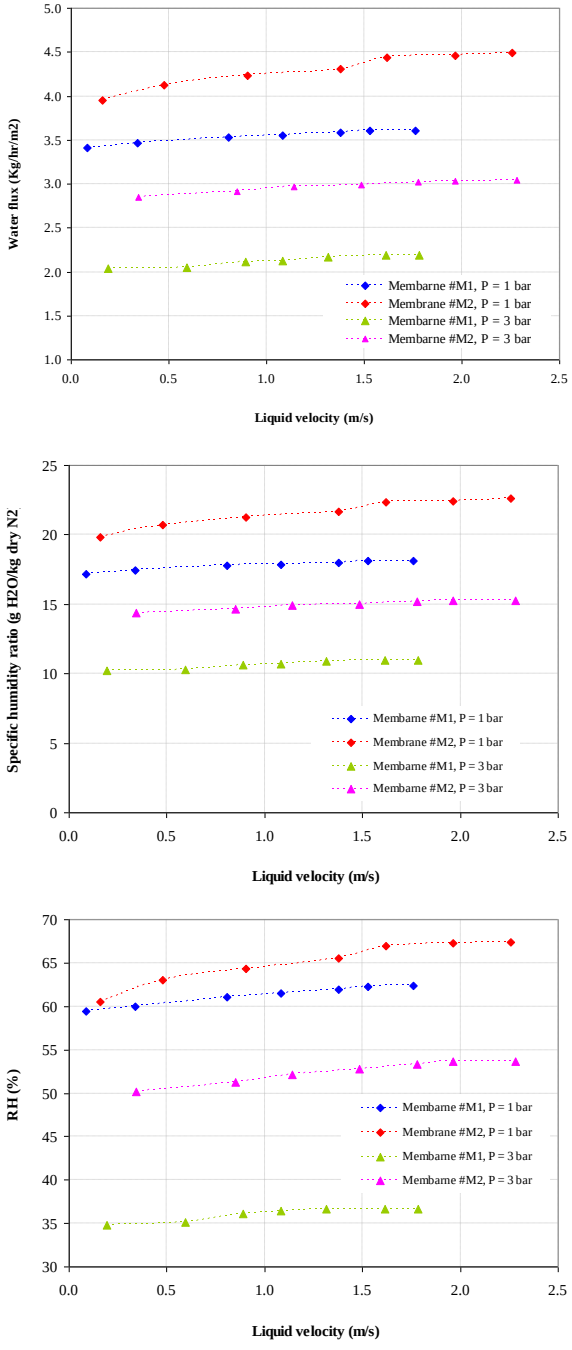

Fig. 6. Plots of water flux, specific humidity ratio and relative humidity of the exit gas at different operating pressures for the fabricated membranes, T = 60 ºC, Q_{gas} = 3 SLPM.

In membrane gas absorption process, the solute gas diffuses through the carrier gas in the pores of the membrane from the gas side to the liquid side while the vapor of liquid absorbent diffuses counter currently from the liquid side to the gas side. The higher the temperature or the lower the boiling point of the liquid absorbent, the higher the concentration of liquid vapor in the pores of the membrane. Therefore, the concentration of the liquid vapor in the pores of the membrane is generally low as the absorption process is commonly done at low temperature.

On the other hand, in the humidification process, the liquid vapor diffuses through the stagnant gas from the liquid side to the gas side and generally the process is done at high temperature to enhance the vapor flux. Therefore, the concentration of the liquid vapor in the pores of the membrane is high and there is more probability for condensation of the vapor in the pores. This event is more pronounced in the narrow parts of the membrane pore as the Kelvin phenomenon reduces the dew point temperature of the water vapor [26].

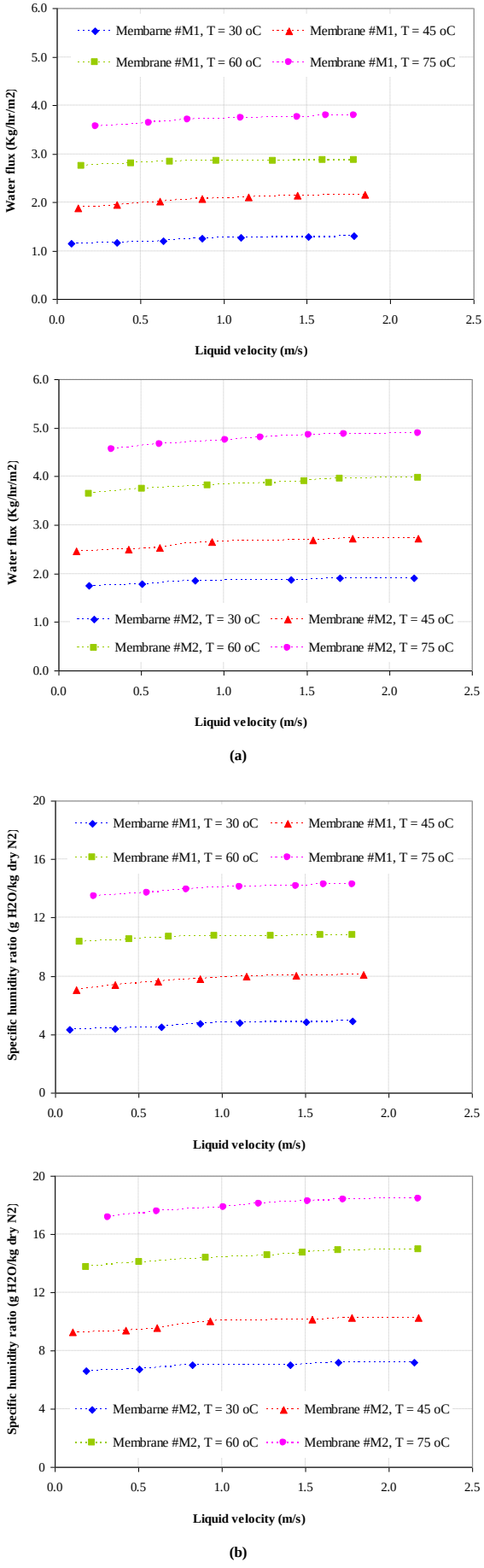

Fig. 7. Plots of (a) water flux, (b) specific humidity ratio and (c) relative humidity of the exit gas at different liquid temperatures for the fabricated membranes, P = 3 bar, Q_{gas} = 4 SLPM.

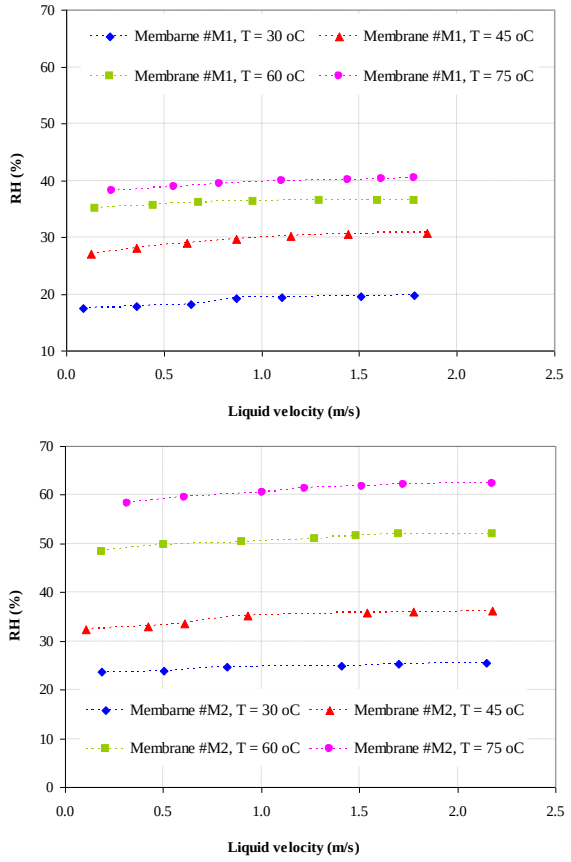

(c)

Fig. 7. Continued.

Furthermore, the higher the surface hydrophilicity of the polymer the more the affinity between the water vapor and the wall of the membrane pores that facilitates the condensation of the water vapor. Referring to Table 5, membrane #M1 has more tortuosity and the hydrophilicity of PES polymer is more than PEI polymer that can cause more condensation of the water vapor along the pores of the membrane and reduction in water flux.

Referring to Figure 6 (effect of operating pressure) and Figure 7 (effect of liquid temperature), as the operating pressure or liquid temperature increases, the difference in water flux between membrane #M2 and membrane #M1 increases that can be related to the effect of the above-mentioned parameters on the condensation of water vapor.

4. Conclusions

Two different PES and PEI hollow fiber membranes were fabricated and their characteristics were investigated by different test methods. In addition, the performance of fabricated membranes in humidification process under various operating conditions was studied where distilled water was sent to the lumen side of the contactor and dry N_2 gas was used as the carrier gas in the shell side of the contactor. The conclusions are as follow:

1) PES membrane has more porous skin layer which its mean pore size and gas permeation rate are 191% and 566% higher than PEI membrane, respectively.
2) The porosity of PEI membrane is higher than PES membrane that can be related to the lower concentration of polymer at the cloud point. Furthermore, the sublayer of PEI membrane shows less spongelike structure.
3) PES membrane has lower wettability even though the mean pore size of PES membrane is more that can be related to its narrower pore size distribution.
4) The water flux of the fabricated membranes increases with liquid velocity, gas flow rate and liquid temperature while operating pressure has opposite effect on the water flux.
5) In all humidification experiments, the water flux of PEI membrane is more than PES membrane that can be related to its lower tortuosity and reduction in vapor condensation along the pore. Furthermore, the difference in water flux between PEI and PES membranes is more as the operating pressure/liquid temperature increases that is related to the enhancement in condensation of water vapor along the pores of the membrane.
6) In humidification process, the structure of membrane sublayer has critical role on the water flux.

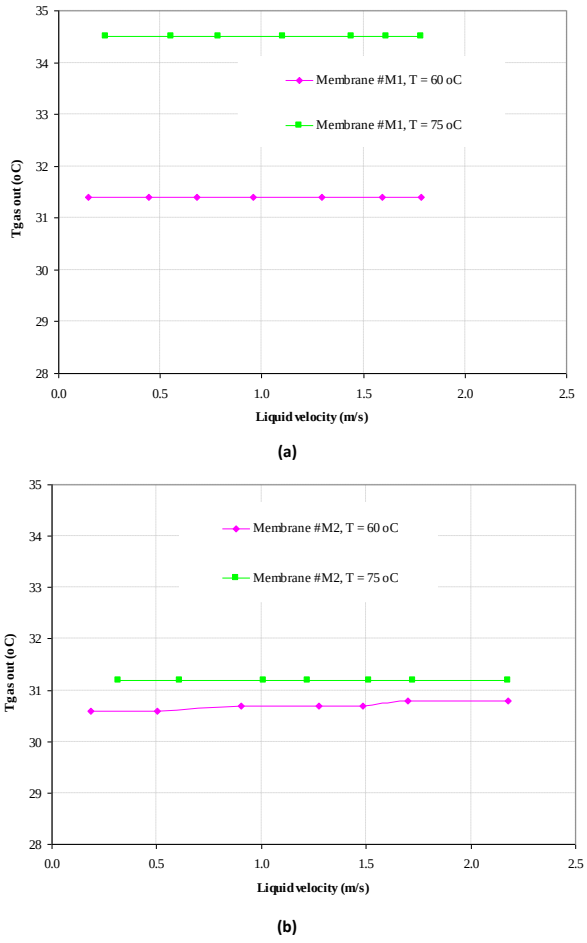

Fig. 8. Temperature plots of the exit gas versus liquid velocity at two different liquid temperatures: (a) membrane #M1 and (b) membrane #M2.

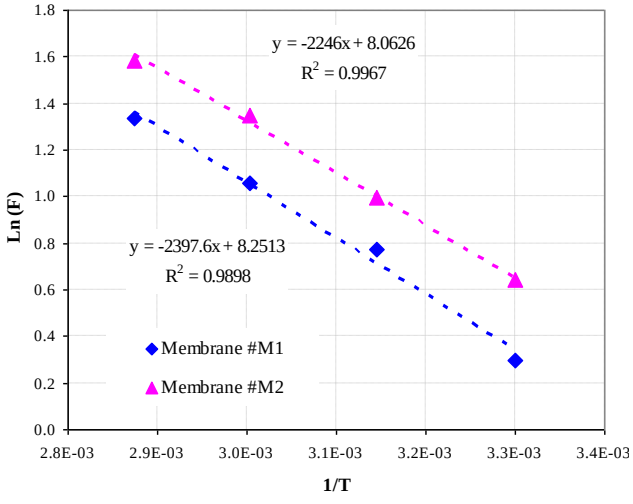

Fig. 9. Plot of Ln F versus $1/T$ for the fabricated membranes at V_{liquid} = 2 m s^{-1}.

References

[1] D. Chu, R.Z. Jiang, Performance of polymer electrolyte membrane fuel cell (PEMFC) stacks, Part I. Evaluation and simulation of an air-breathing PEMFC stack, J. Power Sources 83 (1999) 128-133.

[2] G. Vasu, A.K. Tangirala, B. Viswanathan, K.S. Dhathathreyan, Continuous bubble humidification and control of relative humidity of H_2 for a PEMFC system, Int. J. Hydrogen Energy 33 (2008) 4640-4648.

[3] N.F. Saman, H. Johnstone, Maintaining space temperature and humidity in the digital switch environment, Proceedings of the 16th Annual Industrial Energy Technology Conference, Texas, US, 1994.

[4] A. Traverso, Humidification tower for humid air gas turbine cycles: experimental analysis, Energy 35 (2010) 894-901.

[5] A. Casalegno, S. De Antonellis, L. Colombo, F. Rinaldi, Design of an innovative enthalpy wheel based humidification system for polymer electrolyte fuel cell, Int. J. Hydrogen Energy 36 (2011) 5000-5009.

[6] Z. Xu, Y. Xiao, Y. Wang, Experimental and theoretical studies on air humidification by a water spray at elevated pressure, Appl. Therm. Eng. 27(14) (2007) 2549-2558.

[7] D. Chen, W. Li, H. Peng, An experimental study and model validation of a membrane humidifier for PEM fuel cell humidification control, J. Power Sources 180 (2008) 461-467.

[8] M. Yang, S.M. Huang, X. Yang, Experimental investigations of a quasi-counter flow parallel-plate membrane contactor used for air humidification, Energy Build. 80 (2014) 640-644.

[9] K. Simons, K. Nijmeijer, M. Wessling, Gas-liquid membrane contactors for CO_2 removal, J. Membr. Sci. 340 (2009) 214-220.

[10] Q. Duan, H. Wang, J. Benziger, Transport of liquid water through Nafion membranes, J. Membr. Sci. 392 (2012) 88-94.

[11] S.K. Park, E.A. Cho, I.H. Oh, Characteristics of membrane humidifiers for polymer electrolyte membrane fuel cells, Korean J. Chem. Eng. 22 (2005) 877-881.

[12] J.R. Du, L. Liu, A. Chakma, X. Feng, Using poly(N,N-dimethylaminoethyl methacrylate)/polyacrylonitrile composite membranes for gas dehydration and humidification, Chem. Eng. Sci. 65 (2010) 4672-4681.

[13] A. Samimi, S.A. Mousavi, A. Moallemzadeh, R. Roostaazad, M. Hesampour, A. Pihlajamäki, M. Mänttäri, Preparation and characterization of PES and PSU membrane humidifiers, J. Membr. Sci. 383 (2011) 197-205.

[14] G. Hoogers, Fuel cell technology handbook, CRC Press, Boca Raton, FL, 2003.

[15] S. Park, I.H. Oh, An analytical model of Nafion™ membrane humidifier for proton exchange membrane fuel cells, J. Power Sources 188 (2009) 498-501.

[16] J. Huang, R.J. Cranford, T. Matsuura, C. Roy, Water vapor permeation properties of aromatic polyimides, J. Membr. Sci. 215 (2003) 129-140.

[17] P. Cave, W. Merida, Water flux in membrane fuel cell humidifiers: flow rate and channel location effects, J. Power Sources 175 (2008) 408-418.

[18] L.Z. Zhang, Conjugate heat and mass transfer in heat mass exchanger ducts, Elsevier Publishers Inc., Amsterdam, 2013.

[19] S.K. Park, S.Y. Choe, S. Choi, Dynamic modeling and analysis of a shell-and-tube type gas-to-gas membrane humidifier for PEM fuel cell applications, Int. J. Hydrogen Energy 33 (2008) 2273-2282.

[20] D. Chen, H. Peng, A thermodynamic model of membrane humidifiers for PEM fuel cell humidification control, ASME Journal of Dynamic Systems - Measurement and Control 127 (2005) 424-432.

[21] Gh. Bakeri, S. Naeimifard, T. Matsuura, A.F. Ismail, A porous polyethersulfone hollow fiber membrane in a gas humidification process, RSC Advances 5 (2015) 14448-14457.

[22] D. Kadylak, W. Mérida, Experimental verification of a membrane humidifier model based on the effectiveness method, J. Power Sources 195 (2010) 3166-3175.

[23] K. Ramya, J. Sreenivas, K.S. Dhathathreyan, Study of a porous membrane humidification method in polymer electrolyte fuel cells, Int. J. Hydrogen Energy 36 (2011) 14866-14872.

[24] R. Wang, H.Y. Zhang, P.H.M. Feron, D.T. Liang, Influence of membrane wetting on CO_2 capture in microporous hollow fiber membrane contactors, Sep. Purif. Technol. 46 (2005) 33-40.

[25] Gh. Bakeri, A.F. Ismail, T. Matsuura, Effect of polymer concentration on the structure and performance of polyetherimide hollow fiber membranes, J. Membr. Sci. 363 (2010) 103-111.

[26] Gh. Bakeri, A.F. Ismail, M. Rezaei DashtArzhandi, T. Matsuura, Porous PES and PEI hollow fiber membranes in gas-liquid contacting process - A comparative study, J. Membr. Sci. 475 (2015) 57-64.

[27] G. Bakeri, D. Rana, A.F. Ismail, T. Matsuura, A. Ghaee, Performance of surface-modified poly(etherimide) hollow-fiber membranes in a membrane gas-liquid contacting process with response surface methodology, J. Appl. Polym. Sci. 128 (2013) 1313-1325.

[28] R. Naim, A.F. Ismail, Effect of polymer concentration on the structure and performance of PEI hollow fiber membrane contactor for CO_2 stripping, J. Hazard. Mater. 250-251 (2013) 354-361.

[29] Gh. Bakeri, A.F. Ismail, D. Rana, T. Matsuura, Development of high performance surface modified polyetherimide hollow fiber membrane for gas-liquid contacting processes, Chem. Eng. J. 198-199 (2012) 327-337.

[30] W. Albrecht, Th. Weigel, M. Schossig-Tiedemann, K. Kneifel, K.V. Peinemann, D. Paul, Formation of hollow fiber membranes from poly(ether imide) at wet phase inversion using binary mixtures of solvents for the preparation of the dope, J. Membr. Sci. 192 (2001) 217-230.

[31] L.Z. Zhang, S.M. Huang, Coupled heat and mass transfer in a counter flow hollow fiber membrane module for air humidification, Int. J. Heat Mass Transfer 54 (2011) 1055-1063.

[32] S. Kang, K. Min, S. Yu, Two dimensional dynamic modeling of a shell-and-tube water-to-gas membrane humidifier for proton exchange membrane fuel cell, Int. J. Hydrogen Energy 35 (2010) 1727-1741.